



## Article

# Comparative Analysis of Root Transcriptome of High-NUE Mutant and Wild-Type Barley under Low-Nitrogen Conditions

Runhong Gao <sup>1,2,3</sup> , Longhua Zhou <sup>2,3</sup>, Guimei Guo <sup>2,3</sup>, Yingbo Li <sup>2,3</sup>, Zhiwei Chen <sup>2,3</sup> , Ruiju Lu <sup>2,3</sup>,  
Chenghong Liu <sup>2,3,\*</sup> and Jianmin Chen <sup>1,\*</sup>

<sup>1</sup> Jiangsu Key Laboratories of Crop Genetics and Physiology and Plant Functional Genomics of the Ministry of Education, Co-Innovation Center for Modern Production Technology of Grain Crops of Jiangsu Province, Yangzhou University, Yangzhou 225009, China; gaorunhong@saas.sh.cn

<sup>2</sup> Biotechnology Research Institute, Shanghai Academy of Agricultural Sciences, Shanghai 201106, China; zhoulonghua@saas.sh.cn (L.Z.); guoguimei@saas.sh.cn (G.G.); liyingbo@saas.sh.cn (Y.L.); chenzhiwei@saas.sh.cn (Z.C.); cs7@saas.sh.cn (R.L.)

<sup>3</sup> Shanghai Key Laboratory of Agricultural Genetics and Breeding, Shanghai 201106, China

\* Correspondence: liuchenghong@saas.sh.cn (C.L.); jmchen@yzu.edu.cn (J.C.)

**Abstract:** Although nitrogen (N) deficiency greatly affects N absorption and metabolism in barley, the global transcriptomic changes in morphological and physiological adaptation to altered N availability remains largely unclear. We conducted a comparative transcriptome analysis of roots in A9-29 (low N tolerant line of barley) and Hua 30 (low N-sensitive variety of barley) under low N conditions to elucidate the responses and the underlying molecular mechanism. The results demonstrated that the root architecture was strongly influenced and that the root morphological indexes (total root length, total root area surface, and root volume) were remarkably promoted in A9-29 compared to Hua30 under low N stress. The transcriptome analysis of roots identified 1779 upregulated differentially expressed genes (DEGs) and 1487 downregulated DEGs specifically expressed in A9-29 under low N stress. Specific DEGs in A9-29 were largely enriched in energy metabolism, lipid metabolism, and the metabolism of other amino acids. In addition, transcription factor genes ERFs and IAA-related genes were specifically expressed in A9-29. To conclude, this study could provide a foundation for improving low N tolerance in barley.

**Keywords:** barley (*Hordeum vulgare* L.); low-N stress; root architecture; transcriptome; differentially expressed genes



**Citation:** Gao, R.; Zhou, L.; Guo, G.; Li, Y.; Chen, Z.; Lu, R.; Liu, C.; Chen, J. Comparative Analysis of Root Transcriptome of High-NUE Mutant and Wild-Type Barley under Low-Nitrogen Conditions. *Agronomy* **2023**, *13*, 806. <https://doi.org/10.3390/agronomy13030806>

Academic Editors: Shengguan Cai, Chenchen Zhao and Yuqing Huang

Received: 16 February 2023

Revised: 6 March 2023

Accepted: 8 March 2023

Published: 10 March 2023



**Copyright:** © 2023 by the authors. Licensee MDPI, Basel, Switzerland. This article is an open access article distributed under the terms and conditions of the Creative Commons Attribution (CC BY) license (<https://creativecommons.org/licenses/by/4.0/>).

## 1. Introduction

Nitrogen (N) is one of the major elements and constitutes the driving force for increasing crop yield. The two-fold increase witnessed in agricultural food production worldwide in the past four decades is largely attributed to the seven-fold increase in the application of N fertilizers [1]. With the global food demand estimated to double over the next 50 years, a three-fold increase in global N fertilizer input is anticipated [2]. The indiscriminate use of N fertilizers in agriculture is already exerting and will continue to exert negative effects on the ecological environment [1]. The largest impact would be observed in terms of the eutrophication of freshwater and marine ecosystems due to the leaching of excess nitrogen fertilizers into these water bodies [3]. Therefore, it is necessary to prevent the overuse of nitrogen fertilizers to balance food production and protect environmental health [4]. Moreover, breeding varieties with low-N tolerance, which can decrease N requirements and achieve high yields, will promote green agriculture and sustainable development [5]. Understanding the underlying molecular modulation mechanism of crops under low-N stress is beneficial to improving the tolerance of crops under low-N stress [6].

The proper growth and development of the root system are essential for plants to obtain nutrients and water from different layers of soil [7]. The efficiency of this process

depends on the uptake activity and root architecture, which consequently affects the efficiency of the absorption of N and other elements [8]. Plant roots utilize an “active foraging strategy” to cope with N deficiency through lateral root growth and transcriptome reprogramming [9]. The root architecture is strongly influenced by the availability of N in the soil. Under low-N stress, more photosynthates get transported to roots, resulting in longer root lengths, more fine roots, and deeper root distribution, leading to improved root growth and enhanced nitrogen uptake [10]. Moreover, the development of plant roots is governed by internal regulatory mechanisms [11,12]. Phytohormones are an important component of the internal regulatory mechanism in plant root architecture. It has been demonstrated that nitrogen-induced root architecture remodeling is involved in the cross-regulation of the nitrogen signaling and auxin signaling pathway [13]. Low-N conditions induce the expression of auxin biosynthesis genes, resulting in elevated auxin levels, thereby stimulating lateral root initiation and extension [14]. Abscisic acid (ABA) is a stress hormone and has been implicated in lateral root formation [15,16]. In contrast, cytokinins inhibit lateral root development in an auxin-dependent manner [17]. Ethylene and jasmonate (JA) are integrated into auxin signaling to modulate root development, primarily through transcription factors (TFs) as key crosstalk nodes [18].

Transcription factors (TFs) are central regulators of intrinsic cellular processes, such as differentiation and development, and responses to hormones and environmental factors [19]. In addition, TFs are required for the proper formation of the primary root, root hairs, and lateral roots [20]. TFs involved in modulating root architecture and plasticity primarily include ARF (auxin response factor), WRKY, MYB, bHLH (basic helix–loop–helix), NAC, AP2/ERF (APetala 2/ethylene responsive element-binding factor), MADS, and GRAS, which play different roles in adapting to the changing environment [21].

A previous study has demonstrated that the A9-29 line, a mutant line derived from Hua 30 by microspore EMS (ethyl methane sulfonate) mutagenesis, absorbs nitrogen more efficiently than Hua30 due to the increased nitrogen absorption area, higher nitrogen influx in roots, and enhanced expression of nitrate transport and nitrogen assimilation genes, thereby resulting in more biomass and nitrogen accumulation under low-N conditions [22]. The response and regulatory mechanism underlying the ability of barley roots to cope with low-N stress has remained unclear. Therefore, we conducted a comparative transcriptome analysis of roots in A9-29 (low-N tolerant line) and Hua 30 (low-N sensitive variety) under low-N conditions, which will provide a theoretical foundation for elucidating the regulatory mechanisms of low-N tolerance and breeding low-N-resistant varieties in barley.

## 2. Materials and Methods

### 2.1. Plant Materials and Growth Conditions

Barley Hua30 is a low-N sensitive variety, whereas A9-29 is a mutant obtained from Hua30 by microspore EMS mutagenesis and is a low-N tolerance line with a higher NUE under low-N stress [23]. Seeds were disinfected, rinsed, soaked, and placed on a damp piece of filter paper for germination in culture dishes. After 5 days, the seedlings without seeds were cultivated in water for 2 days and afterward cultured in 10 L of the International Rice Research Institute (IRRI) nutrient solution.  $\text{NH}_4\text{NO}_3$  (0.1 mM) was used as a low-N treatment. The nutrient solution was renewed every 7 days and aerated with an electric pump. The pH was maintained at  $6.2 \pm 0.3$ . There were 27 plants per 10 L of nutrient solution. All the plants were cultivated in a glasshouse (day/night temperature, 20/18 °C; light/dark, 16/8 h; 60% relative humidity) under approximately  $300 \mu\text{mol photon m}^{-2}\text{s}^{-1}$  light intensity. The treatment was performed at 10:00 am. At 0, 7, 14, and 21 days of low-N treatment, the fresh roots were sampled, immediately frozen in liquid nitrogen, and subsequently stored at  $-80 \text{ }^\circ\text{C}$  for further analysis. The samples of six plants from each timepoint were mixed as one replicate, and three replicates of each sample were used for the transcriptome analysis.

## 2.2. Root Morphology

Fresh roots were harvested separately at 0, 7, 14, and 21 days after low-N treatment and separated carefully. Scanned images with a 300 dpi resolution were acquired using a flatbed scanner. The root systems were analyzed by LA-S Plant Root Analysis System (Hangzhou Wseen Detection Technology Co., Ltd., Hangzhou, China) to evaluate the total root length, root surface area, root volume, and root average diameter.

## 2.3. RNA Extraction and Sequencing

The total RNA was extracted from each root sample using mirVana miRNA Isolation Kit according to the manufacturer's instructions. RNA integrity was assessed by Agilent 2100 Bioanalyzer (Agilent Technologies, Santa Clara, CA, USA). The samples with RNA integrity number  $\geq 7$  were used for further analysis. The libraries were constructed using TruSeq Stranded mRNA LT Sample Prep Kit (Illumina, San Diego, CA, USA) following the manufacturer's instructions. The transcriptome sequencing and analysis were conducted by OE Biotech Co., Ltd. (Shanghai, China). Three biological replicates were used for each sample.

## 2.4. RNA-Seq Data Processing and Analysis

The libraries were sequenced on the Illumina HiSeq X Ten platform and generated 150 bp paired-end reads. First, the raw data were processed using the Trimmomatic tool [24] to obtain clean reads. Next, the clean reads were aligned to a barley reference genome using the Hiast2 tool [25]. The fragments per kilo base per million reads (FPKM) value of each gene was calculated using the Cufflinks tool [26], and the read counts of each gene were acquired using HTSeq-count [27]. The differentially expressed genes (DEGs) with  $p < 0.05$  and a foldchange of  $>2$  or  $<0.5$  were identified using the DESeq tool [28]. Short time-series expression miner (STEM) clustering was based on the method described by Ernst and Bar-Joseph [29]. The Gene Ontology (GO) and Kyoto Encyclopedia of Genes and Genomes (KEGG) pathway enrichment analyses of DEGs were performed using the R package.

## 2.5. RT-qPCR Validation

Twelve DEGs were randomly selected and subjected to a quantitative real-time-polymerase chain reaction (qRT-PCR) analysis to verify the data from RNA-seq. The cDNA synthesis and qRT-PCR reaction system were performed according to the method described by Gao et al. [22]. The reference genes were *HvGAPDH* and *HvActin*. Three biological replicates were performed for each treatment. The sequences of primers are shown in Supplementary Table S1.

## 3. Results

### 3.1. Root Morphology Analysis of A9-29 and Hua30 under Low-N Stress

As the low-N culture time increased, the root phenotypes of A9-29 and Hua30 showed a clearly visible difference (Figure S1). The A9-29 and Hua30 samples were then compared for the total root length, total root surface, total root volume, and root average diameter (Figure 1). Compared with Hua30, the total root length and root surface of A9-29 were significantly larger from 7 d to 21 d. The root volume of A9-29 was remarkably greater than that of Hua30 from 14 d to 21 d. The root average diameter decreased with an increase in the treatment time. A9-29 had thinner roots than Hua30; however, a significant difference was observed only at day 7 of low-N stress. These results prove that A9-29 is more tolerant to low-N stress than Hua30.

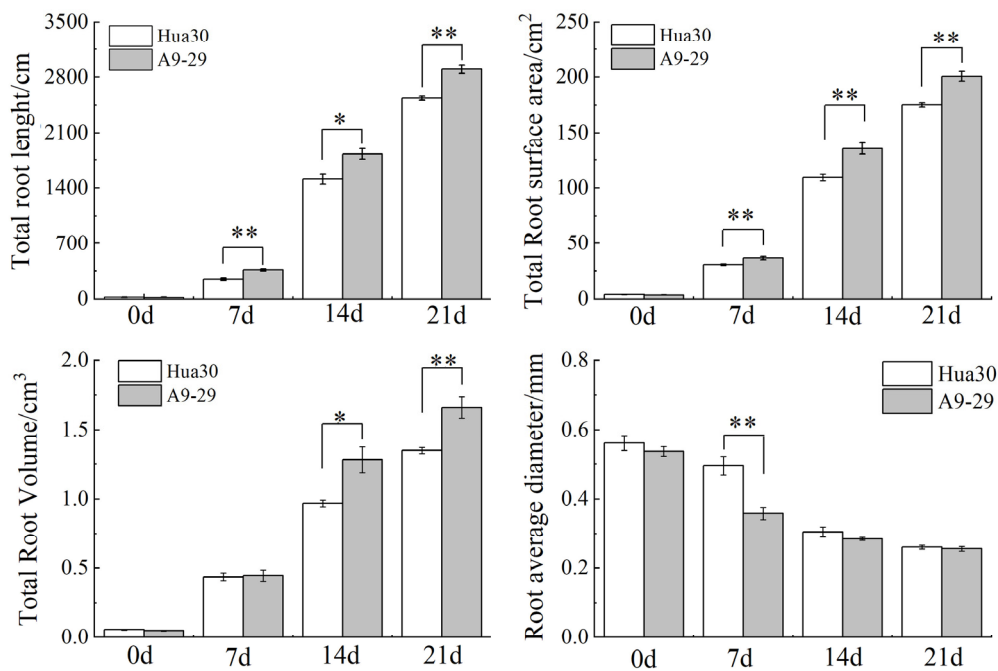


**Figure 1.** Effects of low-N stress on the total root length, total root surface, total root volume, and root average diameter. Values represent the mean  $\pm$  standard deviation (SD) of four replicates. \* or \*\* indicate significant differences in the pair-wise comparisons at  $p < 0.05$  or  $p < 0.01$ .

### 3.2. RNA-Seq Analysis of Roots in A9-29 and Hua30 Subjected to Low-N Stress

An overview of DEGs derived from A9-29 and Hua30 is presented in Figure 2. Compared with the control (0 d), 8251 and 9138 DEGs were found in Hua30 and A9-29 at three-time points under low-N stress, of which 4819 and 5270 DEGs were upregulated and 3702 and 3868 DEGs were downregulated in Hua30 and A9-29 separately (Figure 2A,C,D). The number of DEGs increased with the extension of the low-N treatment time. The number of DEGs in the 21 d sample was nearly two-fold that in the 7 d sample both in Hua30 and A9-29. The number of DEGs in A9-29 was slightly more than that in Hua30, indicating that A9-29 expresses more genes under low-N stress.

Subsequently, the paired comparison was performed in A9-29 and Hua30 at each time point (Figure 2B,E). In total, 1779 upregulated DEGs and 1487 downregulated DEGs were identified in A9-29. Among these, 297 and 318 DEGs were differentially up- or down-regulated at all time points, suggesting that these genes constantly responded to low-N stress in A9-29 during the time course. In addition, different numbers of DEGs displayed time-specific expression, indicating that A9-29 uses a complex process to adapt to low-N stress.

Because the A9-29 was obtained from Hua30 by microspore EMS mutagenesis, the difference between them was a focal point, which should be thoroughly studied in the future.

### 3.3. Functional Annotation of DEGs in A9-29 versus Hua30 under Low-N Stress

To ascertain the biological functions of DEGs in A9-29 and Hua30, we performed a GO enrichment analysis. The DEGs at different time points were divided into three major categories, including 38 functional groups (Figure S2). In the biological process category, numerous DEGs were found to be associated with a metabolic process, cellular process, and single-organism process. The dominant terms in the cellular components were cell, cell part, and membrane. In the molecular function category, the majority of the DEGs were related to binding and catalytic activity (Figure 3). Moreover, signaling and response to stimulus in the biological process category and antioxidant activity in the molecular function category were functionally annotated, proving their vital functions in the stress tolerance of plants. The biological processes were further divided into upregulated and downreg-

ulated groups (Figure 4). The figure depicts the degree to which the selected biological processes were overrepresented among the DEGs in A9-29 and Hua30 at each time point. In the upregulated groups, protein phosphorylation was enriched from 14 d to 21 d. The majority of the metabolic process, response to stress, response to water, chitin catabolic process, and cell wall macromolecule catabolic process were enriched at 7 d and 21 d. The phosphatidylinositol phosphorylation was enriched at 21 d. In the downregulated groups, protein phosphorylation was found to be enriched from 0 d to 14 d. The oxidation–reduction process, malate transportation, and heme oxidation were enriched at 0 d. The cellular amino acid metabolic process and the carboxylic acid metabolic process were enriched at 14 d. Interestingly, the up-regulated biological processes displayed a higher degree of enrichment than the down-regulated ones, indicating that the upregulated biological processes were involved in positive functions in A9-29 under low-N stress.

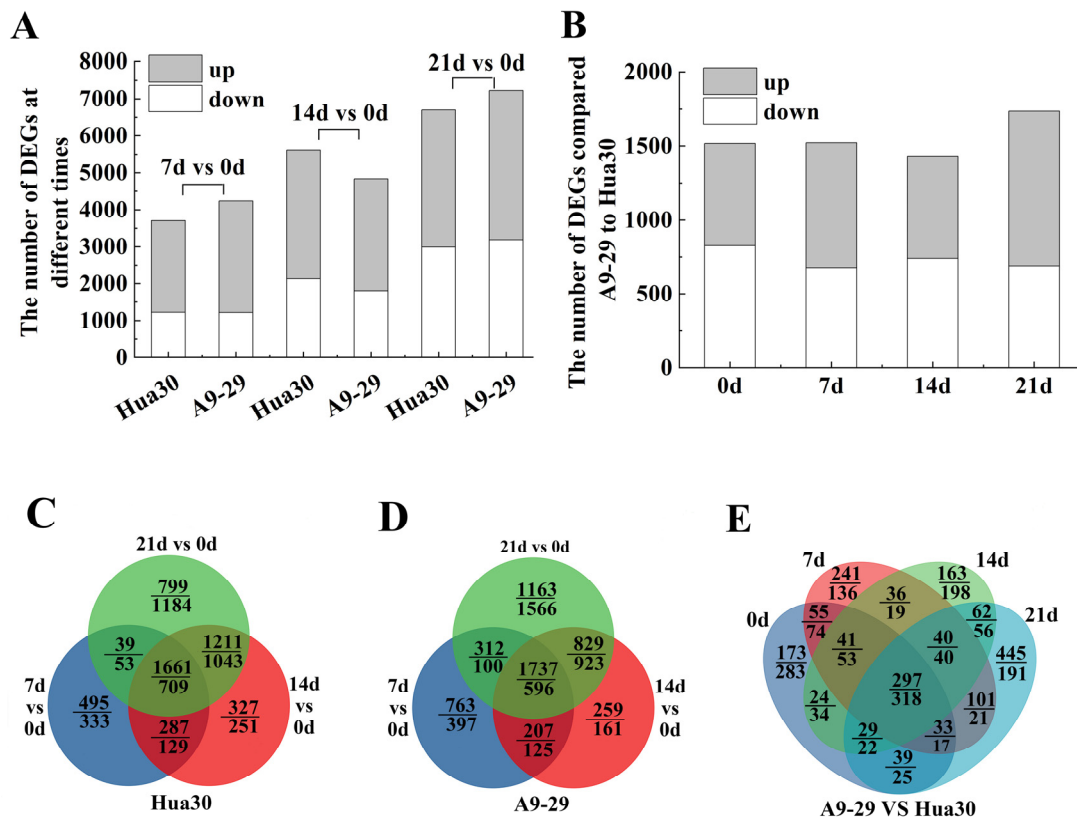


**Figure 2.** Venn diagrams of DEGs between A9-29 and Hua30 under low-N conditions. (A) Summary of DEGs in Hua30 and A9-29 at each time point compared to those at 0d. (B) Summary of DEGs in A9-29 compared to Hua30. (C) The numbers of up- and down-regulated DEGs in Hua30 under low-N stress. (D) The numbers of up- and downregulated DEGs in A9-29 under low-N stress. (E) The numbers of up- and downregulated DEGs in A9-29 compared to Hua30. The numbers above the horizontal line indicate the number of upregulated DEGs and those below the horizontal line represent the number of downregulated DEGs.

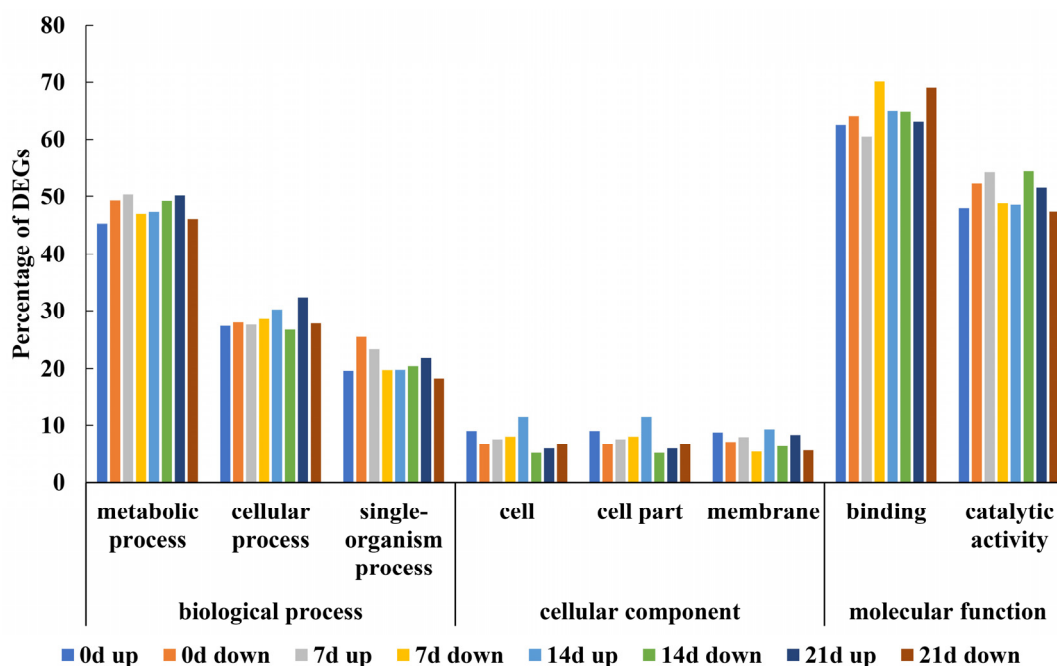


**Figure 3.** Major GO analysis of DEGs at different time points in each category. Metabolic process, cellular process, and single-organism process belong to the biological process category. Cell, cell part, and membrane belong to the cellular component category. Binding and catalytic activity belong to the molecular function category.

### 3.4. Functional Analysis of KEGG Pathway of DEGs in A9-29 versus Hua30 under Low-N Stress

To explore the biological pathway triggered by low-N stress in A9-29 versus Hua30, all DEGs were functionally annotated in the KEGG database. DEGs with significant matches were assigned to 53, 42, 49, and 47 KEGG pathways at 0, 7, 14, and 21 d, respectively, under low-N stress. Among these pathways, 19 KEGG pathways were identified at all time points, 20 KEGG pathways were found at three of the four time points, and 12 KEGG pathways were recognized at two of the four time points. Finally, 11, 4, 10, and 6 KEGG pathways were identified as unique to one of the four time points. These pathways were divided into four categories, namely, metabolism, cellular processes, environmental information processing, and genetic information processing, which were further divided into 17 subcategories (Figure 5). Numerous DEGs were functionally enriched in the category metabolism. The top four subcategories in the metabolism category were biosynthesis of other secondary metabolites, energy metabolism, metabolism of other amino acids, and amino acid metabolism. Moreover, DEGs were functionally enriched in xenobiotic biodegradation and metabolism, carbohydrate metabolism, and lipid metabolism, which were intricately related to the plant response to environmental stress, as well as growth and development regulation. In addition, 17 DEGs were functionally enriched in the subcategory cell growth and death, which belonged to cellular processes. Similarly, 25 DEGs were classified into four subcategories, belonging to genetic information processing, and all DEGs were down-regulated. In total, 42 DEGs were classified into two subcategories including membrane transport and signal transduction, belonging to environmental information processing. Among these subcategories, energy metabolism, lipid metabolism, and metabolism of other amino acid were of concern due to the fact that the number of upregulated DEGs was more than twice that of the downregulated ones. Subsequently, five major KEGG pathways were significantly enriched in A9-29 compared to Hua30 (Table 1), suggesting that the genes involved in these pathways may be associated with different responses to low-N stress of the two barley lines.

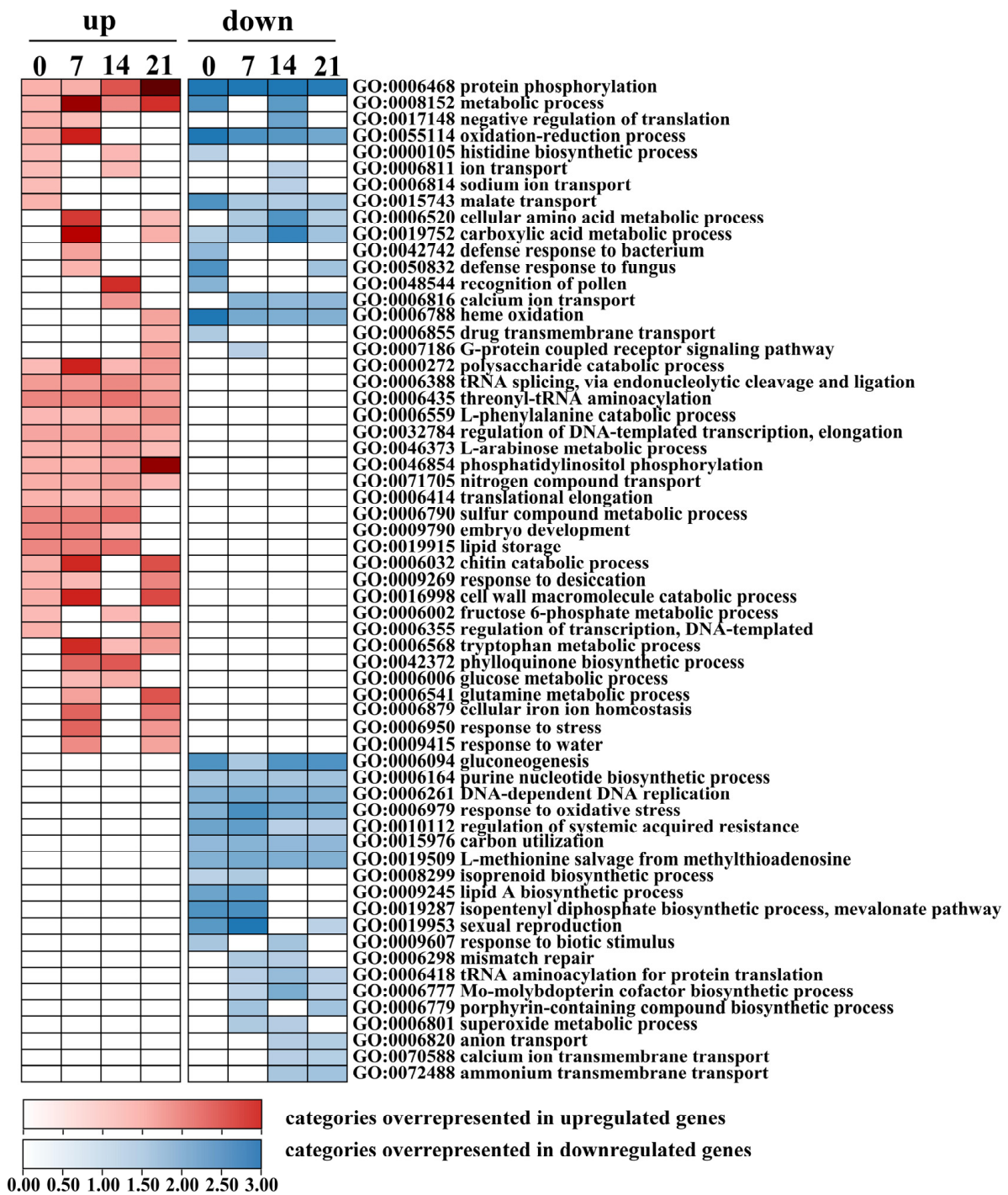


**Figure 4.** The biological process of GO categories in time course comparisons between A9-29 and Hua30. The categories are remarkably enriched ( $p < 0.05$ ) in either upregulated or downregulated genes. Negative  $\log_{10}$  ( $p$ -value) was performed for each category enrichment test and subsequently plotted for each time point.

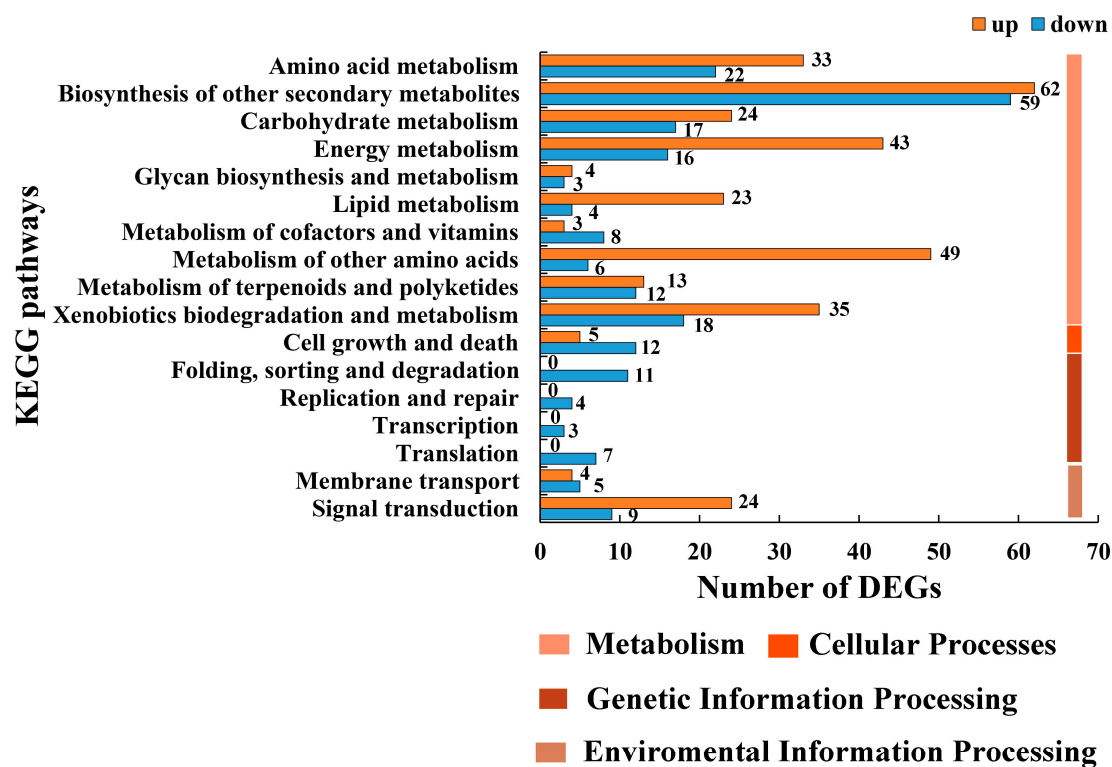


**Figure 5.** KEGG pathway enrichment analysis of DEGs at all time points in A9-29 versus Hua30 under low-N stress.

**Table 1.** The major KEGG pathway enrichment for upregulated DEGs in A9-29 versus Hua30 under low-N stress.

KEGG Pathway	Description	−Log <sub>10</sub> (p Value)			
		0 d	7 d	14 d	21 d
Energy metabolism					
ko00910	Nitrogen metabolism	1.43			1.64
ko00920	Sulfur metabolism	6.04	6.69	3.93	2.35
Lipid metabolism					
ko00073	Cutin, suberine, and wax biosynthesis	1.99	1.51	1.91	2.83
ko01040	Biosynthesis of unsaturated fatty acids	1.66	1.77	2.27	1.69
Metabolism of other amino acids					
ko00480	Glutathione metabolism		4.34		13.26

### 3.5. DEGs Involved in Nitrogen/Sulfur Metabolism and Other Types of Nutrient Uptake under Low-N Stress in A9-29

Nitrogen metabolism is an essential plant biological process which greatly affects the growth and development of plants. Compared to Hua30, five DEGs were up-regulated and involved in the nitrogen metabolism pathway in A9-29. *HORVU6Hr1G005590*, a high-affinity nitrate transporter 2.6 gene (*NRT2.6*) was upregulated in A9-29 from 0 d to 14 d under low-N stress. Two carbonic anhydrases (*HORVU7Hr1G020190* and *HORVU7Hr1G020370*), a formamidase (*HORVU3Hr1G074250*), and a cyanate lyase (*HORVU4Hr1G076970*), which could catalyze different substrates to ammonia, as a source of nitrogen, were upregulated in A9-29.

Eleven DEGs were up-regulated and involved in sulfur metabolism. A ferredoxin-sulfite reductase (*HORVU0Hr1G026700*) catalyzes the reduction of sulfite to sulfide and subsequently participates in the biosynthesis of sulfur-containing amino acids and cofactors. A sulfur dioxygenase (*HORVU3Hr1G060920*) is known to regulate sulfide levels in living



organisms. A 3'(2'),5'-bisphosphate nucleotidase (*HORVU7Hr1G021700*) has been reported to convert the adenosine 3'-phosphate 5'-phosphosulfate to adenosine 5'-phosphosulfate, thereby controlling the sulfur flux in the sulfur activation pathway. Three cysteine synthases (*HORVU2Hr1G000260*, *HORVU7Hr1G023500*, and *HORVU3Hr1G047030*) catalyze O-acetylserine and sulfide to form cysteine. Similarly, five cystathionine gamma-synthases (*HORVU2Hr1G011930*, *HORVU2Hr1G011970*, *HORVU4Hr1G028560*, *HORVU4Hr1G028570*, and *HORVU4Hr1G028580*) catalyze sulfide to L-cysteine. These genes participate in sulfate assimilation and sulfur-containing amino acid metabolism. In addition, a sulfate transporter 3.1 (*HORVU3Hr1G068140*) was up-regulated in A9-29.

In addition to nitrate and sulfate transporters, several DEGs encoding other nutrient transporters were identified in A9-29, such as potassium transporter (8), zinc transporter (4), iron transporter (5), magnesium transporter (2), boron transporter (1), and sugar transporter (9) (Table S2). The majority of these DEGs were up-regulated in A9-29, indicating that the A9-29 sample had a higher nutrient uptake capacity under the low-N condition. Moreover, these nutrients were affected by N metabolism under cross-talking regulation.

### 3.6. DEGs Involved in Lipid Metabolism under Low-N Stress in A9-29

Two major KEGG pathways were involved in lipid metabolism. Four very-long-chain 3-oxoacyl-CoA reductases (*HORVU7Hr1G001550*, *HORVU7Hr1G044900*, *HORVU7Hr1G063290*, and *HORVU1Hr1G045230*), a very-long-chain enoyl-CoA reductase (*HORVU1Hr1G013970*), a peroxisomal acyl-coenzyme A oxidase 1 (*HORVU1Hr1G028500*), a 3-oxoacyl-[acyl-carrier protein] reductase (*HORVU3Hr1G006910*), and a acyl-[acyl-carrier-protein] desaturase (*HORVU5Hr1G039730*) participated in the biosynthesis of unsaturated fatty acids. Two peroxygenases (*HORVU2Hr1G088760* and *HORVU6Hr1G073690*) and four fatty acyl-CoA reductases (*HORVU3Hr1G002120*, *HORVU7Hr1G020270*, *HORVU7Hr1G059000*, and *HORVU7Hr1G092230*) participated in cutin, suberine, and wax biosynthesis.

### 3.7. DEGs Involved in Glutathione Metabolism under Low-N Stress in A9-29

Thirty DEGs encoding glutathione-S transferase (GST) identified in A9-29 under low-N stress were involved in glutathione metabolism. A heat map of these genes was constructed by  $\text{Log}_2(\text{FPKM}+1)$  for Hua30 and A9-29 at four time points (Figure 6). These DEGs displayed more transcript accumulation in A9-29 than in Hua30 especially at 21 d.

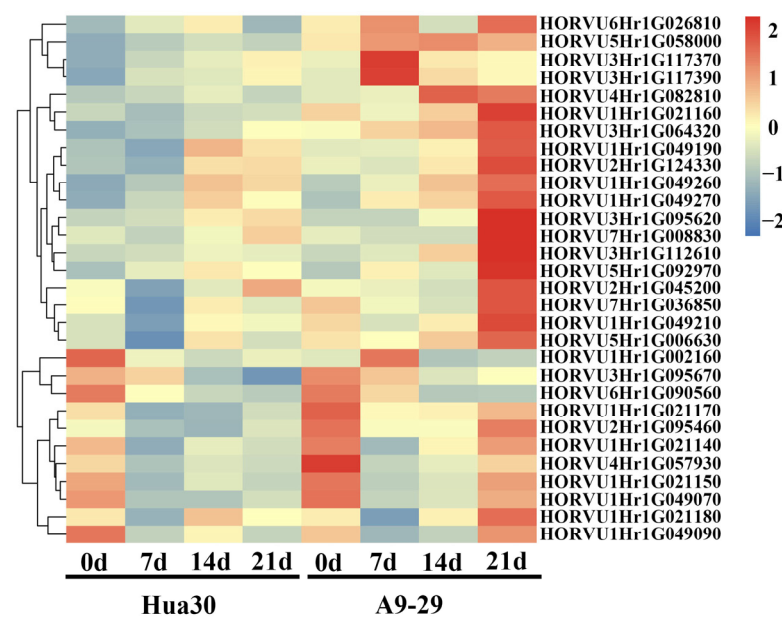
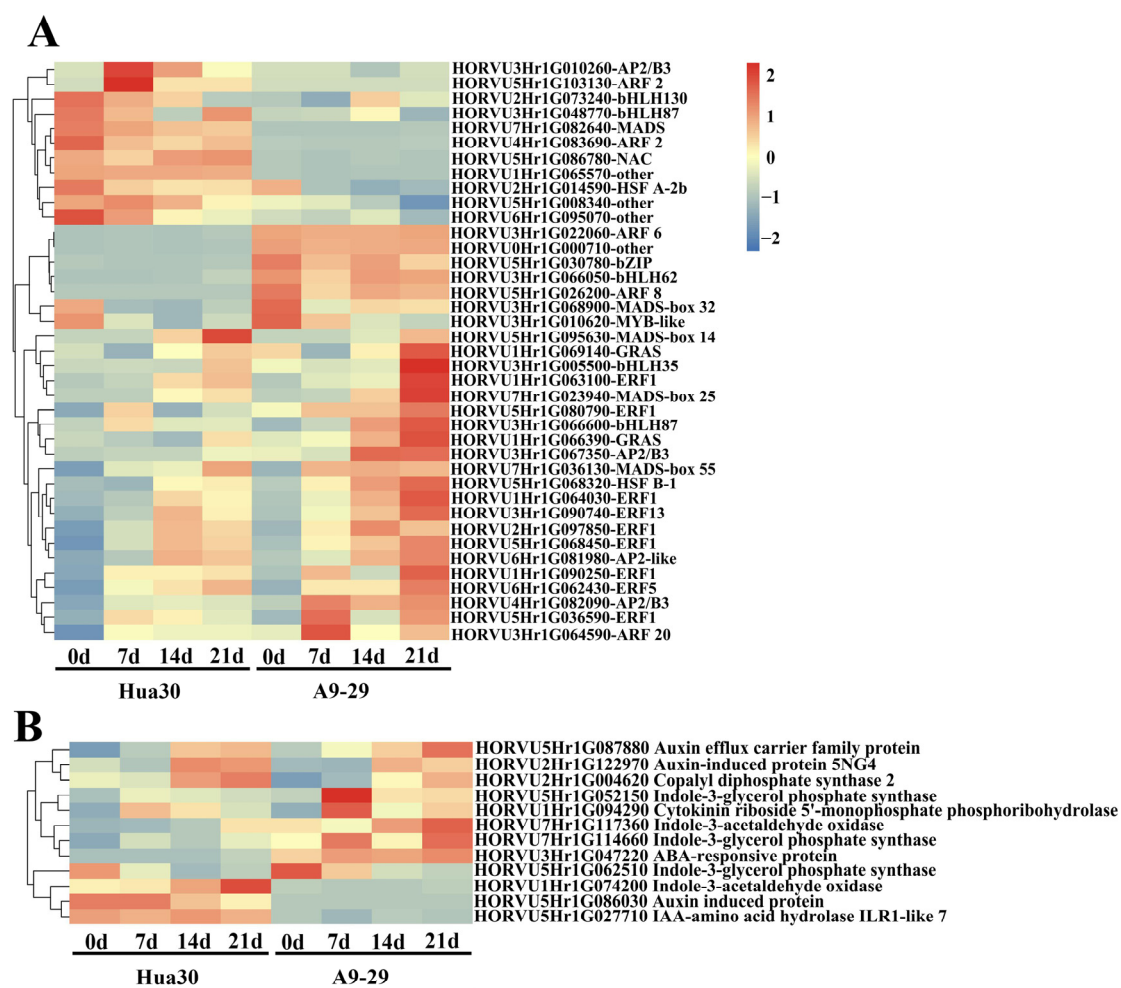


Figure 6. The average linkage hierarchical cluster analysis of DEGs encoding GSTs.

### 3.8. Transcription Factors

It is well known that N deficiency response is regulated at the transcriptional level. Several transcriptional factor genes were identified from the DEGs. In total, 97 DEGs encoding TFs were identified in A9-29 compared with Hua30 under low-N stress (Table S3). Among the 97 DEGs, 39 DEGs were significantly regulated at two or more time points and these were selected for the average linkage hierarchical cluster analysis (Figure 7A). These TFs belonged to different families, such as AP2 (4), ARF (5), ERF (9), MYB-like (1), HSF (2), bHLH (5), bZIP (1), NAC (1), MADS-box (5), GRAS (2), and others (4). The results showed that 28 DEGs were upregulated in A9-29, especially from 14 d to 21 d, and only 11 DEGs were upregulated in Hua30. All the ERFs and GRAS displayed more upregulation in A9-29 compared with Hua30, implying these TFs have positive functions in A9-29 against N deficiency. In addition, ERFs and ARFs were involved in plant hormone signal pathways.



**Figure 7.** The average linkage hierarchical cluster analysis of DEGs encoding transcription factors (A). Hormone signaling-related DEGs (B).

### 3.9. DEGs Involved in Phytohormones

Phytohormones regulate plant morphogenesis in response to external stimuli, including nutrient stress. Thirty-nine hormone-signaling-related DEGs were identified in A9-29 compared with Hua30 under low-N stress, including auxin (IAA, 23), gibberellin (GA, 7), cytokinin (CTK, 3), ethylene (ETH, 4), and abscisic acid (ABA, 2) (Table S4). In addition, 12 of 39 hormone-signaling-related DEGs were significantly regulated at two or more time points which were selected for the average linkage hierarchical cluster analysis (Figure 7B). Among these 12 DEGs, 9 DEGs were involved in auxin signal transduction,

strongly suggesting that auxin signaling plays an important function in A9-29 to promote root development in response to N deficiency.

### 3.10. Expression Pattern of DEGs between A9-29 and Hua30 throughout Low-N Process

The DEGs identified in A9-29 and Hua30 under low-N stress were assigned to different temporal expression profiles based on the pattern of expression by STEM. The cluster analysis revealed 12 significant expression profiles in Hua30 and A9-29, respectively (Figure 8). The expression patterns of DEGs in profiles 42, 49, 48, 29, and 18 presented an increasing trend under low-N stress, whereas those in profiles 9, 1, 12, and 23, showed a decreasing trend in both A9-29 and Hua30. Compared with Hua 30, profiles 40 and 46 showed increasing trends and profile 11 showed a decreasing trend, which was significantly identified only in A9-29. The GO functional enrichment analysis indicated that DEGs in profile 40 were remarkably enriched in the protein modification process, transportation, the regulation of gene expression, the metabolic process, catalytic activity, and binding. The DEGs in profile 46 were significantly enriched in the oxidation–reduction process, the response to stress, protein phosphorylation, the metabolic process, transportation, and binding. The DEGs in profile 11 were highly enriched in microtubule-based movement, cell wall, the response to oxidative stress, the metabolic process, and binding. In contrast, profiles 45, 47, and 0 were significantly identified only in Hua30. The DEGs in profiles 45 and 47 were first upregulated, and then downregulated. These genes were predicted to be largely in charge of protein phosphorylation, the response to oxidative stress, the membrane, protein kinase activity, and binding. GO enrichments for profile 0 showing decreasing trends included those in transmembrane transportation, the regulation of transcription, mitochondrion, and binding.

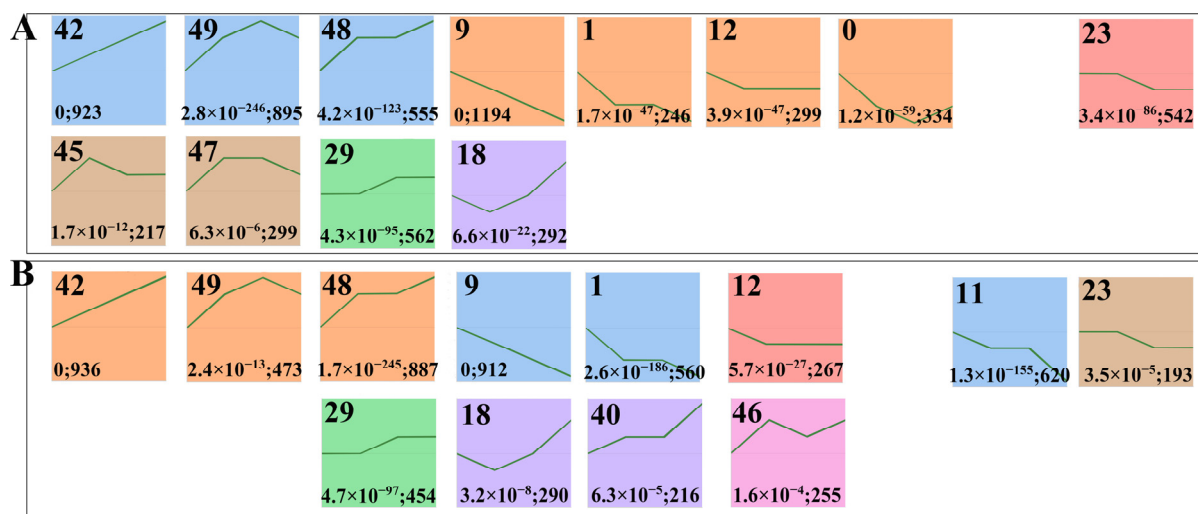


**Figure 8.** Clustering results of time course data from Hua30 (A) and A9-29 (B) roots based on STEM analysis. Different model temporal expression profiles correspond to different boxes. The profile ID number is displayed in the top left corner of each box. The *p*-value and gene numbers assigned to the profiles are shown at the bottom left corner of each box separated by a semicolon. The green curve represents a model expression pattern.

The cluster analysis manifested that more DEGs in the Hua30 sample showed a reduction in transcript abundance from 14 d to 21 d. In contrast, more DEGs were upregulated in the A9-29 sample from 14 d to 21 d. These upregulated genes at the later stages of treatment may likely function in A9-29 under low-N stress.

### 3.11. Validation of RNA-Seq Gene Expression

Twelve representative DEGs were randomly selected for qRT-PCR to confirm the data obtained from the RNA-seq. These DEGs include one nitrate transporter 1:2 (*HORVU1Hr1G050540*), one high affinity nitrate transporter 2.6 (*HORVU6Hr1G005590*), one potassium transporter family protein (*HORVU1Hr1G009100*), one NAC domain containing protein 2 (*HORVU3Hr1G062150*), two transcription factors including bHLH62 (*HORVU3Hr1G066050*), and zinc finger CCCH domain-containing protein 14 (*HORVU6Hr1G033840*), one GST family protein (*HORVU1Hr1G021170*), one caffeic acid 3-O-methyltransferase 1 (*HORVU3Hr1G006050*), one 23 kDa jasmonate-induced protein (*HORVU3Hr1G117640*), one ATP-dependent 6-phosphofructokinase 3 (*HORVU7Hr1G047000*), one E3 ubiquitin-protein ligase SINA-like 7 (*HORVU0Hr1G006120*), and one germin-like protein 4 (*HORVU4Hr1G005440*). As shown by the result, an excellent agreement was achieved between the RNA-seq data and qRT-PCR data of the selected genes ( $R^2 = 0.90$ ) (Figure 9), indicating the reliability of the RNA-seq data.

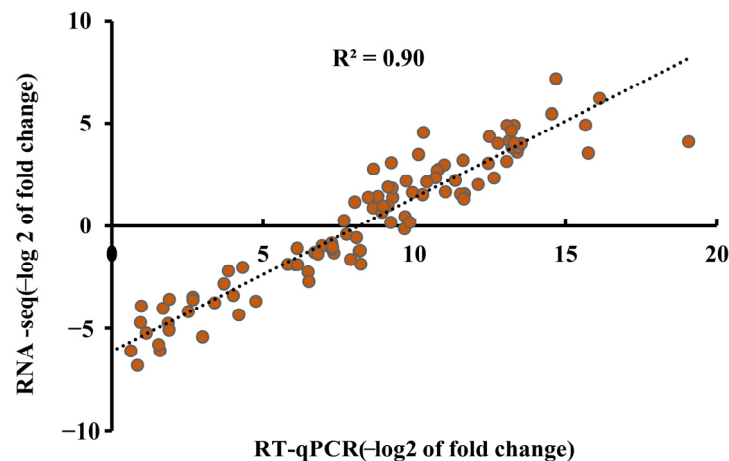


**Figure 9.** Validation of RNA-seq data by qRT-PCR. Scatter plots represent the transcriptional changes revealed by qRT-PCR analysis and RNA-seq by negative log<sub>2</sub> of fold change.

## 4. Discussion

Plants respond to N deficiency through numerous morphological and physiological responses. The morphological features of roots, the primary organ of N absorption, determine the ability of plants to obtain N from soil [30]. Root morphology significantly varies in response to different levels of N availability among the genotypes of crops, such as *Arabidopsis* [31], cotton [32], and wheat [33]. Under N-deficient conditions, high N efficiency genotypes can create more root dry biomass than genotypes with low-N efficiency can. The morphological traits of roots in N-efficient genotypes were significantly higher in number than in inefficient genotypes under N-deficient conditions, thus facilitating more N capture [32]. As mentioned in Section 3, the A9-29 sample showed a greater induction of root morphological traits under a low-N concentration, indicating that the A9-29 sample was more tolerant to the low-N concentration than the Hua30 sample was. Ultimately, longer root length, increased root surface, and higher root volume were observed in the A9-29 sample compared to the Hua30 sample, implying that A9-29 roots have a greater absorption area than Hua30 roots do and therefore can obtain more N nutrients and efficiently adapt to low-N conditions.

Plant nitrogen metabolism is a highly complex process. Plants have evolved multiple mechanisms to regulate N metabolism to counter various levels of N availability and environmental stress [34]. Although high-affinity nitrate transport genes (*NRT2s*) have been reported to be remarkably expressed in N-deficient seedlings [35], this was not detected in this experiment. In our previous work, the high-affinity nitrate transport genes were expressed more in A9-29 than in Hua30 [22]. In this experiment, only *HvNRT2.6* was

dramatically expressed in A9-29 compared to Hua30. A likely explanation is that day 0 was used as a control in this experiment instead of day 1, which was the control in the previous work, causing variations in nitrogen availability throughout the treatment process. The N availability to the seedlings in this experiment was changed from zero at 0 d to the peak at 7 d, followed by decreasing it to almost zero. Some research shows that the expression of *NRT2.1* was different between nitrogen starvation and low-N concentration treatments of wheat roots [36,37]. Furthermore, it was reported that the *AtNRT2.6* gene was involved in the response to biotic and abiotic stresses [38,39]. Moreover, the *NRT2.6* gene expression is induced by high nitrogen levels [38]. It has been demonstrated that the *NRT2.5/NRT2.6*-dependent plant signaling pathway and the nitrate-dependent regulation of root development are independent [40]. Hence, the functions of *NRT2.6* in response to N deficiency in A9-29 warrant further investigation. Most genes related to N metabolism were undetectable, suggesting that A9-29 and Hua30 tried to keep a normal N metabolism while adapting to low-N stress.

Nitrogen and sulfur are assimilated by plants primarily into proteins. The amount of sulfur required by a plant is strongly dependent on its N nutrition [41]. Sulfur metabolism is a crucial part of essential amino acid components of cysteine and methionine. In addition, it is associated with the production of several secondary metabolites, including H<sub>2</sub>S, glutathione, polysulfides, and polysulfanes, which are known to increase tolerance to biotic and abiotic stresses [42]. During the N deficiency treatment, sulfur metabolism was enriched in A9-29 compared to Hua30, implying that sulfur metabolism exerts a positive function in A9-29 against N deficiency.

Plant lipids' functions as a hydrophobic barrier to membranes and also as signaling molecules that regulate cell metabolism are critical for maintaining the integrity of cells and organelles [43]. Unsaturated fatty acids (UFAs), primarily C18 species, are deeply linked to both abiotic and biotic stresses. Moreover, C18 UFAs have multiple functions, including their role as precursors for multiple bioactive molecules, stocks of extracellular barrier components, and intrinsic antioxidants [44]. Cutin and suberin play important roles in adjusting plant morphology and protecting plants from adversity stresses [45]. In this experiment, two lipid metabolism pathways, including the biosynthesis of unsaturated fatty acids and the biosynthesis of cutin, suberin, and wax, were enriched in A9-29 compared to Hua30 under N deficiency, indicating the presence of a concerted effort in A9-29 to adapt to high levels of N stress to promote root growth.

Low or excessive amounts of essential nutrients could cause oxidative damage to plants, resulting in reduced production [46]. As a macronutrient, appropriate N levels are conducive to normal plant growth, whereas N starvation or excess can make plants suffer from N stress. Under N-deficient conditions, stress response pathways have been employed to regulate root growth in response to N starvation [47]. Glutathione is an essential ingredient of the defense system in plants and animals [48], which not only plays a redox role in plant adaptation to stress conditions but is also implicated in plant development and stress tolerance [49]. In addition, glutathione metabolism plays an essential role in deciding the level of expression of defense-related genes under environmental stresses [50]. High levels of glutathione can cause stress tolerance and translational changes [51]. GSTs are multifunctional enzymes that use glutathione as a co-substrate or co-enzyme to perform a range of functional roles [52]. In plants, several GSTs are involved in important physiological activities, such as environmental stress management, phytohormone signaling, cell death, and several others [53]. GSTs can eliminate reactive oxygen species and lipid hydroperoxides via antioxidant reactions [54]. We found that the glutathione metabolism pathway and the GST genes significantly contributed to low N condition in A9-29 compared with Hua30, indicating they play vital roles in A9-29 to reduce the stress caused by low-N concentration.

Phytohormones are critical factors in modulating the responses of root morphogenesis to different environmental conditions, including N availability [55]. Several studies have demonstrated that N and phytohormone signals are integrated to promote plant morpho-

logical and physiological adaptation to tolerate both N deficiency or excess [9,56,57]. Auxin is a major regulator of root growth and the N-mediated root architecture [58]. There exists a strong relationship between the stimulation of root growth by low nitrate and increased IAA contents in roots [59]. IAA could integrate with N signaling to regulate root growth in response to variations in N availability [47]. As shown in Figure 7, IAA related genes are specifically expressed in A9-29, indicating that this phytohormone can sense the variations in N availability and modulate root growth.

TFs are the master regulators of stress response genes, and are promising targets for genetic improvement in abiotic stress tolerance in crops [19,60]. ERFs serve as a key regulatory hub, integrating hormone and redox signaling in response to different abiotic stresses [61]. Moreover, *ERF1* plays an active function in abiotic stresses by integrating ET, ABA, and JA signaling through specific stress gene regulation [62]. Overexpression of the *TaERF1* gene has been reported to improve the tolerance to multiple stresses in transgenic wheat [63]. The *TdERF1* gene may provide a discriminating marker between salt-tolerant and sensitive durum wheat varieties [64]. Here, seven ERF1s of nine ERFs were identified in A9-29, indicating that ERF1s may have functions under low-N stress in A9-29. It is yet to be studied whether ERF1 can be used as a marker to identify A9-29 and Hua30 roots.

In summary, we deduced the mechanism underlying the low-N tolerance of A9-29. More energy production and stronger stress resistance could promote growth performance in the root morphological traits of A9-29, enhancing the absorption of increased amounts of N nutrients under low-N conditions. The DEGs involved in energy metabolism, lipid metabolism, and the metabolism of other amino acids could play vital roles in tolerating low-N stress in A9-29. Furthermore, certain phytohormone- and TF-related DEGs were altered to activate the corresponding signaling pathways and regulate root growth in response to low-N stress.

## 5. Conclusions

Low-N stress could significantly affect the architecture of the root system. Compared to Hua30, A9-29 has a longer root length, extended root area surface and root volume, and more fine roots under low-N stress. The transcriptome analysis of the roots identified 1779 upregulated DEGs and 1487 downregulated DEGs that were differentially expressed in A9-29 response to low-N stress. Specific DEGs in A9-29 are primarily enriched in energy metabolism, lipid metabolism, and the metabolism of other amino acids. ERF transcription factor gene families and IAA-related genes were specifically expressed in A9-29. These related genes may modulate root growth and morphology to tolerate low-N stress. These findings will enhance our understanding of barley response mechanisms under low-N conditions.

**Supplementary Materials:** The following supporting information can be downloaded at: <https://www.mdpi.com/article/10.3390/agronomy13030806/s1>. Table S1: List of genes and primers selected for q-PCR validation. Table S2: DEGs encoding the others nutrient transporters identified in A9-29 compared with Hua30 under long-term LN stress. Table S3: DEGs encoding transcription factors (TFs) were identified in A9-29 compared with Hua30 under long-term LN stress. Table S4: The hormone signaling-related DEGs were identified in A9-29 compared with Hua30 under long-term LN stress. Figure S1: The root phenotypes of Hua 30 and A9-29 at different time points under low-N conditions. Figure S2: GO analysis of DEGs in each category. (A) Biological process. (B) Cellular component. (C) Molecular function. The number on the X-axis indicates different GO terms as follows: 1—metabolic process; 2—cellular process; 3—single-organism process; 4—biological regulation; 5—regulation of biological process; 6—localization; 7—establishment of localization; 8—response to stimulus; 9—multicellular organismal process; 10: cellular component organization or biogenesis; 11—developmental process; 12—signaling; 13—multi-organism process; 14—negative regulation of biological process; 15—reproduction; 16—reproductive process; 17—immune system process; 18—cell; 19—cell part; 20—membrane; 21—membrane part; 22—organelle; 23—organelle part; 24—macromolecular complex; 25—extracellular region; 26—membrane-enclosed lumen; 27—extracellular region part; 28—binding; 29—catalytic activity; 30—transporter activity;

31—antioxidant activity; 32—nucleic acid binding transcription factor activity; 33—nutrient reservoir activity; 34—electron carrier activity; 35—enzyme regulator activity; 36—structural molecule activity; 37—molecular transducer activity; 38—receptor activity. The Y-axis indicates the percentage of DEGs.

**Author Contributions:** Conceptualization, R.G., J.C. and C.L.; data curation, R.G., Y.L. and Z.C.; formal analysis, G.G.; funding acquisition, R.L. and C.L.; investigation, R.G., L.Z. and G.G.; methodology, R.G. and L.Z.; project administration, C.L.; supervision, R.L., J.C. and C.L.; validation, R.G., Y.L. and Z.C.; writing—original draft, R.G.; writing—review and editing, R.L., J.C. and C.L. All authors have read and agreed to the published version of the manuscript.

**Funding:** This research was funded by the National Natural Science Foundation of China, grant number 31801353; China Agriculture Research System of MOF and MARA, grant number CARS-05-01A-02; and the SAAS program for Excellent Research Team, grant number 2022018.

**Data Availability Statement:** The RNA-seq data have been deposited with the National Center for Biotechnology Information: BioProject ID PRJNA934683.

**Conflicts of Interest:** The authors declare no conflict of interest. The funder played no role in the design of the study, in the collection, analyses or interpretation of the data, in the writing of the manuscript, or in the decision to publish the results.

## References

- Hirel, B.; Le Gouis, J.; Ney, B.; Gallais, A. The challenge of improving nitrogen use efficiency in crop plants: Towards a more central role for genetic variability and quantitative genetics within integrated approaches. *J. Exp. Bot.* **2007**, *58*, 2369–2387. [[CrossRef](#)]
- Tilman, D.; Cassman, K.G.; Matson, P.A.; Naylor, R.; Polasky, S. Agricultural sustainability and intensive production practices. *Nature* **2002**, *418*, 671. [[CrossRef](#)] [[PubMed](#)]
- Tilman, D.; Balzer, C.; Hill, J.; Befort, B.L. Global food demand and the sustainable intensification of agriculture. *Proc. Natl. Acad. Sci. USA* **2011**, *108*, 20260–20264. [[CrossRef](#)] [[PubMed](#)]
- Li, D.; Tian, M.; Cai, J.; Jiang, D.; Cao, W.; Dai, T. Effects of low nitrogen supply on relationships between photosynthesis and nitrogen status at different leaf position in wheat seedlings. *Plant Growth Regul.* **2013**, *70*, 257–263. [[CrossRef](#)]
- Liu, C.; Gong, X.; Wang, H.; Dang, K.; Deng, X.; Feng, B. Low-nitrogen tolerance comprehensive evaluation and physiological response to nitrogen stress in broomcorn millet (*Panicum miliaceum* L.) seedling. *Plant Physiol. Biochem.* **2020**, *151*, 233–242. [[CrossRef](#)]
- Yang, Y.; Gao, S.; Su, Y.; Lin, Z.; Guo, J.; Li, M.; Wang, Z.; Que, Y.; Xu, L. Transcripts and low nitrogen tolerance: Regulatory and metabolic pathways in sugarcane under low nitrogen stress. *Environ. Exp. Bot.* **2019**, *163*, 97–111. [[CrossRef](#)]
- Giehl, R.F.H.; Gruber, B.D.; von Wirén, N. It's time to make changes: Modulation of root system architecture by nutrient signals. *J. Exp. Bot.* **2014**, *65*, 769–778. [[CrossRef](#)]
- Kiba, T.; Krapp, A. Plant nitrogen acquisition under low availability: Regulation of uptake and root architecture. *Plant Cell Physiol.* **2016**, *57*, 707–714. [[CrossRef](#)]
- Ruffel, S.; Krouk, G.; Ristova, D.; Shasha, D.; Birnbaum, K.D.; Coruzzi, G.M. Nitrogen economics of root foraging: Transitive closure of the nitrate-cytokinin relay and distinct systemic signaling for N supply vs. demand. *Proc. Natl. Acad. Sci. USA* **2011**, *108*, 18524–18529. [[CrossRef](#)]
- Wang, Y.; Zhang, X.; Chen, J.; Chen, A.; Wang, L.; Guo, X.; Niu, Y.; Liu, S.; Mi, G.; Gao, Q. Reducing basal nitrogen rate to improve maize seedling growth, water and nitrogen use efficiencies under drought stress by optimizing root morphology and distribution. *Agric. Water Manag.* **2019**, *212*, 328–337. [[CrossRef](#)]
- Wu, B.; Ren, W.; Zhao, L.; Li, Q.; Sun, J.; Chen, F.; Pan, Q. Genome-Wide Association Study of Root System Architecture in Maize. *Genes* **2022**, *13*, 181. [[CrossRef](#)] [[PubMed](#)]
- Kong, X.; Zhang, M.; De Smet, I.; Ding, Z. Designer crops: Optimal root system architecture for nutrient acquisition. *Trends Biotechnol.* **2014**, *32*, 597–598. [[CrossRef](#)]
- Chaiwanon, J.; Wang, W.; Zhu, J.Y.; Oh, E.; Wang, Z.Y. Information integration and communication in plant growth regulation. *Cell* **2016**, *164*, 1257–1268. [[CrossRef](#)]
- Hu, S.; Zhang, M.; Yang, Y.; Xuan, W.; Zou, Z.; Arkorful, E.; Chen, Y.; Ma, Q.; Jeyaraj, A.; Chen, X.; et al. A novel insight into nitrogen and auxin signaling in lateral root formation in tea plant [*Camellia sinensis* (L.) O. Kuntze]. *BMC Plant Biol.* **2020**, *20*, 232. [[CrossRef](#)]
- Signora, L.; De Smet, I.; Foyer, C.H.; Zhang, H. ABA plays a central role in mediating the regulatory effects of nitrate on root branching in *Arabidopsis*. *Plant J.* **2001**, *28*, 655–662. [[CrossRef](#)] [[PubMed](#)]
- De Smet, I.; Zhang, H.; Inze, D.; Beeckman, T. A novel role for abscisic acid emerges from underground. *Trends Plant Sci.* **2006**, *11*, 434–439. [[CrossRef](#)]

17. Laplaze, L.; Benkova, E.; Casimiro, I.; Maes, L.; Vanneste, S.; Swarup, R.; Weijers, D.; Calvo, V.; Parizot, B.; Herrera-Rodriguez, M.B.a.; et al. Cytokinins act directly on lateral root founder cells to inhibit root initiation. *Plant Cell* **2007**, *19*, 3889–3900. [[CrossRef](#)]
18. Xu, P.; Zhao, P.X.; Cai, X.T.; Mao, J.L.; Miao, Z.Q.; Xiang, C.B. Integration of jasmonic acid and ethylene into auxin signaling in root development. *Front. Plant Sci.* **2020**, *11*, 271. [[CrossRef](#)]
19. Baillo, E.H.; Kimotho, R.N.; Zhang, Z.; Xu, P. Transcription factors associated with abiotic and biotic stress tolerance and their potential for crops improvement. *Genes* **2019**, *10*, 771. [[CrossRef](#)]
20. Montiel, G.; Gantet, P.; Jay-Allemand, C.; Breton, C. Transcription factor networks. Pathways to the knowledge of root development. *Plant Physiol.* **2004**, *136*, 3478–3485. [[CrossRef](#)]
21. Perotti, M.F.; Arce, A.L.; Ariel, F.D.; Figueroa, C.M.; Chan, R.L. The transcription factor AtHB23 modulates starch turnover for root development and plant survival under salinity. *Environ. Exp. Bot.* **2022**, *201*, 104994. [[CrossRef](#)]
22. Gao, R.; Guo, G.; Xu, H.; Chen, Z.; Li, Y.; Lu, R.; Liu, C.; Chen, J. Enhancement of root architecture and nitrate transporter gene expression improves plant growth and nitrogen uptake under long-term low-nitrogen stress in barley (*Hordeum vulgare* L.) seedlings. *Plant Growth Regul.* **2021**, *95*, 343–353. [[CrossRef](#)]
23. Gao, R.; Guo, G.; Fang, C.; Huang, S.; Chen, J.; Lu, R.; Huang, J.; Fan, X.; Liu, C. Rapid generation of barley mutant lines with high nitrogen uptake efficiency by microspore mutagenesis and field screening. *Front. Plant Sci.* **2018**, *9*, 450. [[CrossRef](#)]
24. Bolger, A.M.; Lohse, M.; Usadel, B. Trimmomatic: A flexible trimmer for Illumina sequence data. *Bioinformatics* **2014**, *30*, 2114–2120. [[CrossRef](#)]
25. Kim, D.; Langmead, B.; Salzberg, S.L. HISAT: A fast spliced aligner with low memory requirements. *Nat. Methods* **2015**, *12*, 357–360. [[CrossRef](#)] [[PubMed](#)]
26. Trapnell, C.; Williams, B.A.; Pertea, G.; Mortazavi, A.; Kwan, G.; van Baren, M.J.; Salzberg, S.L.; Wold, B.J.; Pachter, L. Transcript assembly and quantification by RNA-Seq reveals unannotated transcripts and isoform switching during cell differentiation. *Nat. Biotechnol.* **2010**, *28*, 511–515. [[CrossRef](#)]
27. Anders, S.; Pyl, P.T.; Huber, W. HTSeq—A Python framework to work with high-throughput sequencing data. *Bioinformatics* **2015**, *31*, 166–169. [[CrossRef](#)]
28. Anders, S.; Huber, W. Differential expression of RNA-Seq data at the gene level—The DESeq package. *Heidelb. Ger. Eur. Mol. Biol. Lab.* **2012**, *10*, f1000research.
29. Ernst, J.; Bar-Joseph, Z. STEM: A tool for the analysis of short time series gene expression data. *BMC Bioinform.* **2006**, *7*, 191. [[CrossRef](#)] [[PubMed](#)]
30. Jiang, S.; Sun, J.; Tian, Z.; Hu, H.; Michel, E.J.S.; Gao, J.; Jiang, D.; Cao, W.; Dai, T. Root extension and nitrate transporter up-regulation induced by nitrogen deficiency improves nitrogen status and plant growth at the seedling stage of winter wheat (*Triticum aestivum* L.). *Environ. Exp. Bot.* **2017**, *141*, 28–40. [[CrossRef](#)]
31. Gruber, B.D.; Giehl, R.F.; Friedel, S.; von Wiren, N. Plasticity of the *Arabidopsis* root system under nutrient deficiencies. *Plant Physiol.* **2013**, *163*, 161–179. [[CrossRef](#)] [[PubMed](#)]
32. Iqbal, A.; Qiang, D.; Zhun, W.; Xiangru, W.; Huiping, G.; Hengheng, Z.; Nianchang, P.; Xiling, Z.; Meizhen, S. Growth and nitrogen metabolism are associated with nitrogen-use efficiency in cotton genotypes. *Plant Physiol. Biochem.* **2020**, *149*, 61–74. [[CrossRef](#)] [[PubMed](#)]
33. Sinha, S.K.; Kumar, A.; Tyagi, A.; Venkatesh, K.; Paul, D.; Singh, N.K.; Mandal, P.K. Root architecture traits variation and nitrate-influx responses in diverse wheat genotypes under different external nitrogen concentrations. *Plant Physiol. Biochem.* **2020**, *148*, 246–259. [[CrossRef](#)] [[PubMed](#)]
34. Wang, M.; Shen, Q.; Xu, G.; Guo, S. New insight into the strategy for nitrogen metabolism in plant cells. *Int. Rev. Cell Mol. Biol.* **2014**, *310*, 1–37. [[CrossRef](#)]
35. Guo, T.; Xuan, H.; Yang, Y.; Wang, L.; Wei, L.; Wang, Y.; Kang, G. Transcription analysis of genes encoding the wheat root transporter NRT1 and NRT2 families during nitrogen starvation. *J. Plant Growth Regul.* **2014**, *33*, 837–848. [[CrossRef](#)]
36. Yin, L.-P.; Li, P.; Wen, B.; Taylor, D.; Berry, J.O. Characterization and expression of a high-affinity nitrate system transporter gene (*TaNRT2.1*) from wheat roots, and its evolutionary relationship to other *NTR2* genes. *Plant Sci.* **2007**, *172*, 621–631. [[CrossRef](#)]
37. Sinha, S.K.; Tyagi, A.; Mandal, P.K. External Nitrogen and Carbon Source-Mediated Response on Modulation of Root System Architecture and Nitrate Uptake in Wheat Seedlings. *J. Plant Growth Regul.* **2019**, *38*, 283–297. [[CrossRef](#)]
38. Dechorgnat, J.; Patriot, O.; Krapp, A.; Fagard, M.; Daniel-Vedele, F. Characterization of the *Nrt2.6* gene in *Arabidopsis thaliana*: A link with plant response to biotic and abiotic stress. *PLoS ONE* **2012**, *7*, e42491. [[CrossRef](#)]
39. Mantelin, S.; Desbrosses, G.; Larcher, M.; Tranbarger, T.J.; Cleyet-Marel, J.C.; Touraine, B. Nitrate-dependent control of root architecture and N nutrition are altered by a plant growth-promoting *Phyllobacterium* sp. *Planta* **2006**, *223*, 591–603. [[CrossRef](#)]
40. Kechid, M.; Desbrosses, G.; Rokhsi, W.; Varoquaux, F.; Djekoun, A.; Touraine, B. The *NRT2.5* and *NRT2.6* genes are involved in growth promotion of *Arabidopsis* by the plant growth-promoting rhizobacterium (PGPR) strain *Phyllobacterium brassicacearum* STM196. *New Phytol.* **2013**, *198*, 514–524. [[CrossRef](#)]
41. Rennenberg, H. The fate of excess sulfur in higher plants. *Annu. Rev. Plant Physiol.* **1984**, *35*, 121–153. [[CrossRef](#)]
42. Fuentes-Lara, L.O.; Medrano-Macias, J.; Perez-Labrada, F.; Rivas-Martinez, E.N.; Garcia-Enciso, E.L.; Gonzalez-Morales, S.; Juarez-Maldonado, A.; Rincon-Sanchez, F.; Benavides-Mendoza, A. From elemental sulfur to hydrogen sulfide in agricultural soils and plants. *Molecules* **2019**, *24*, 2282. [[CrossRef](#)]
43. Kim, H.U. Lipid metabolism in plants. *Plants* **2020**, *9*, 871. [[CrossRef](#)] [[PubMed](#)]



44. He, M.; Qin, C.X.; Wang, X.; Ding, N.Z. Plant unsaturated fatty acids: Biosynthesis and regulation. *Front. Plant Sci.* **2020**, *11*, 390. [[CrossRef](#)] [[PubMed](#)]
45. Pollard, M.; Beisson, F.; Li, Y.; Ohlrogge, J.B. Building lipid barriers: Biosynthesis of cutin and suberin. *Trends Plant Sci.* **2008**, *13*, 236–246. [[CrossRef](#)]
46. Chen, W.; Xiangpeng, L.; Wenyong, Z.; Jinggui, F. The regulatory and signaling roles of glutathione in modulating abiotic stress responses and tolerance. In *Glutathione in Plant Growth, Development, and Stress Tolerance*; Hossain, M.A., Mostofa, M.G., Diaz-Vivancos, P., Burritt, D.J., Fujita, M., Tran, L.-S.P., Eds.; Springer International Publishing: Cham, Switzerland, 2017; Volume 7, pp. 147–169. [[CrossRef](#)]
47. Luo, J.; Zhou, J.; Li, H.; Shi, W.; Polle, A.; Lu, M.; Sun, X.; Luo, Z.B. Global poplar root and leaf transcriptomes reveal links between growth and stress responses under nitrogen starvation and excess. *Tree Physiol.* **2015**, *35*, 1283–1302. [[CrossRef](#)] [[PubMed](#)]
48. Hameed, A.; Sharma, I.; Kumar, A.; Azooz, M.M.; Ahmad Lone, H.; Ahmad, P. Glutathione metabolism in plants under environmental stress. In *Oxidative Damage to Plants*; Ahmad, P., Ed.; Academic Press: Salt Lake City, UT, USA, 2014; Volume 6, pp. 183–200. [[CrossRef](#)]
49. Gong, B.; Sun, S.; Yan, Y.; Jing, X.; Shi, Q. Glutathione metabolism and its function in higher plants adapting to stress. In *Antioxidants and Antioxidant Enzymes in Higher Plants*; Gupta, D., Palma, J., Corpas, F., Eds.; Springer International Publishing: Cham, Switzerland, 2018; Volume 9, pp. 181–205. [[CrossRef](#)]
50. Cao, F.; Fu, M.; Wang, R.; Diaz-Vivancos, P.; Hossain, M.A. Exogenous glutathione-mediated abiotic stress tolerance in plants. In *Glutathione in Plant Growth, Development, and Stress Tolerance*; Hossain, M.A., Mostofa, M.G., Diaz-Vivancos, P., Burritt, D.J., Fujita, M., Tran, L.-S.P., Eds.; Springer International Publishing: Cham, Switzerland, 2017; Volume 8, pp. 171–194. [[CrossRef](#)]
51. Cheng, M.C.; Ko, K.; Chang, W.L.; Kuo, W.C.; Chen, G.H.; Lin, T.P. Increased glutathione contributes to stress tolerance and global translational changes in *Arabidopsis*. *Plant J.* **2015**, *83*, 926–939. [[CrossRef](#)]
52. Dixon, D.P.; Laphorn, A.; Edwards, R. Plant glutathione transferases. *Genome Biol.* **2002**, *3*, reviews3004. [[CrossRef](#)]
53. Vaish, S.; Gupta, D.; Mehrotra, R.; Mehrotra, S.; Basantani, M.K. Glutathione S-transferase: A versatile protein family. *3 Biotech* **2020**, *10*, 321. [[CrossRef](#)]
54. Gullner, G.; Komives, T.; Kiraly, L.; Schroder, P. Glutathione S-transferase enzymes in plant-pathogen interactions. *Front. Plant Sci.* **2018**, *9*, 1836. [[CrossRef](#)]
55. Krouk, G. Hormones and nitrate: A two-way connection. *Plant Mol. Biol.* **2016**, *91*, 599–606. [[CrossRef](#)]
56. Kiba, T.; Kudo, T.; Kojima, M.; Sakakibara, H. Hormonal control of nitrogen acquisition: Roles of auxin, abscisic acid, and cytokinin. *J. Exp. Bot.* **2011**, *62*, 1399–1409. [[CrossRef](#)]
57. Krouk, G.; Ruffel, S.; Gutiérrez, R.A.; Gojon, A.; Crawford, N.M.; Coruzzi, G.M.; Lacombe, B. A framework integrating plant growth with hormones and nutrients. *Trends Plant Sci.* **2011**, *16*, 178–182. [[CrossRef](#)]
58. Mohd-Radzman, N.A.; Djordjevic, M.A.; Imin, N. Nitrogen modulation of legume root architecture signaling pathways involves phytohormones and small regulatory molecules. *Front. Plant Sci.* **2013**, *4*, 385. [[CrossRef](#)]
59. Tian, Q.; Chen, F.; Liu, J.; Zhang, F.; Mi, G. Inhibition of maize root growth by high nitrate supply is correlated with reduced IAA levels in roots. *J. Plant Physiol.* **2008**, *165*, 942–951. [[CrossRef](#)]
60. Woodrow, P.; Pontecorvo, G.; Ciarmiello, L.F.; Annunziata, M.G.; Fuggi, A.; Carillo, P. Transcription factors and genes in abiotic stress. In *Crop Stress and Its Management: Perspectives and Strategies*; Venkateswarlu, B., Shanker, A.K., Shanker, C., Maheswari, M., Eds.; Springer: Dordrecht, The Netherlands, 2012; Volume 9, pp. 317–357. [[CrossRef](#)]
61. Müller, M.; Munné-Bosch, S. Ethylene Response Factors: A key regulatory hub in hormone and stress signaling. *Plant Physiol.* **2015**, *169*, 32–41. [[CrossRef](#)]
62. Cheng, M.C.; Liao, P.M.; Kuo, W.W.; Lin, T.P. The *Arabidopsis* ETHYLENE RESPONSE FACTOR1 regulates abiotic stress-responsive gene expression by binding to different cis-acting elements in response to different stress signals. *Plant Physiol.* **2013**, *162*, 1566–1582. [[CrossRef](#)]
63. Xu, Z.-S.; Xia, L.-Q.; Chen, M.; Cheng, X.-G.; Zhang, R.-Y.; Li, L.-C.; Zhao, Y.-X.; Lu, Y.; Ni, Z.-Y.; Liu, L.; et al. Isolation and molecular characterization of the *Triticum aestivum* L. ethylene-responsive factor 1 (*TaERF1*) that increases multiple stress tolerance. *Plant Mol. Biol.* **2007**, *65*, 719–732. [[CrossRef](#)]
64. Makhloufi, E.; Yousfi, F.E.; Marande, W.; Mila, I.; Hanana, M.; Berges, H.; Mzid, R.; Bouzayen, M. Isolation and molecular characterization of ERF1, an ethylene response factor gene from durum wheat (*Triticum turgidum* L. subsp. *durum*), potentially involved in salt-stress responses. *J. Exp. Bot.* **2014**, *65*, 6359–6371. [[CrossRef](#)]

**Disclaimer/Publisher’s Note:** The statements, opinions and data contained in all publications are solely those of the individual author(s) and contributor(s) and not of MDPI and/or the editor(s). MDPI and/or the editor(s) disclaim responsibility for any injury to people or property resulting from any ideas, methods, instructions or products referred to in the content.